

Electronic Supplementary Information (ESI)

Elucidating Organ-Specific Metabolic Toxicity Chemistry from Electrochemiluminescent Enzyme/DNA Arrays and Bioreactor Bead-LC-MS/MS

Dhanuka P. Wasalathanthri, Dandan Li, Donghui Song, Zhifang Zheng, Dharamainder Choudhary, Ingela Jansson, Xiuling Lu, John B. Schenkman, James F. Rusling*

SUPPORTING INFORMATION

Chemicals and materials

[Ru(bpy)₂(PVP)₁₀]²⁺ (Ru^{II}PVP (bpy = 2,2-bipyridyl; PVP = poly(4-vinylpyridine)) was synthesized and characterized as described previously.¹ Styrene (M_w= 104.15), 2-Acetylaminofluorene (2-AAF, M_w= 223.27), 4-(Methylnitrosamino)-1-(3-pyridyl)-1-butanone (NNK, M_w= 207.23), poly(diallyldimethylammonium chloride) (PDDA, average M_w= 100,000-200,000), poly(sodium 4-styrenesulfonate) (PSS, average M_w= 70000), calf thymus DNA (Type I) and all other chemicals were from Sigma. Pooled male human liver microsomes (Liver, 20 mg mL⁻¹ in 250 mM sucrose) contained (a) 20 mg mL⁻¹ total protein content, (b) total cyt P450 content of 340 pmol mg⁻¹ of protein using the method of Omura and Sato,² baculovirus-insect cell expressed cyt P450 1B1 supersomes (cyt P450 1B1), 4.5 mg/ml in 100mM potassium phosphate buffer of pH 7.4 with representative total cyt P450 content of 220 pmol mg⁻¹ of protein; baculovirus-insect cell expressed cyt P450 1A1 supersomes (cyt P450 1A1), 5.0 mg/ml in 100mM potassium phosphate buffer of pH 7.4 with representative total cyt P450 content of 120 pmol mg⁻¹ of protein; baculovirus-insect cell expressed cyt P450 3A4 supersomes (cyt P450 3A4), 5.0 mg/ml in 100mM potassium phosphate buffer of pH 7.4 with representative total cyt P450 content of 200 pmol mg⁻¹ of protein; and baculovirus-insect cell expressed cyt P450 3A5 supersomes (cyt P450 3A5), 14 mg/ml in 100mM potassium phosphate buffer of pH 7.4 with representative total cyt P450 content of 1000 pmol mg⁻¹ of protein; were from BD Gentest (Woburn, MA). Human lung microsomes (Lung), 10 mg mL⁻¹ in 250 mM sucrose; Human intestinal microsomes (Intestine), 20 mg mL⁻¹ in 250 mM sucrose; Human kidney microsomes (Kidney), 10 mg mL⁻¹ in 250 mM sucrose; Human liver cytosol (HLC), 20 mg mL⁻¹ in 50 mM Tris 150 mM KCl, 2 mM EDTA of pH 7.5; Human lung cytosol (HLuC), 12.1 mg mL⁻¹ in 250 mM sucrose; Human intestinal cytosol (HIC), 11.7 mg mL⁻¹ in 250 mM sucrose; Human kidney cytosol (HKC), 10.6 mg mL⁻¹ in 250 mM sucrose were purchased from Celsis (Chicago, IL).

Fluidic set up

The fluidic chip (Scheme S1) consists of a top poly(methylmethacrylate) (PMMA) plate featuring an optical glass window, Pt counter and Ag/AgCl reference electrode wires in the bottom side, a silicone rubber gasket, the microwell printed PG chip, a Cu plate underneath the

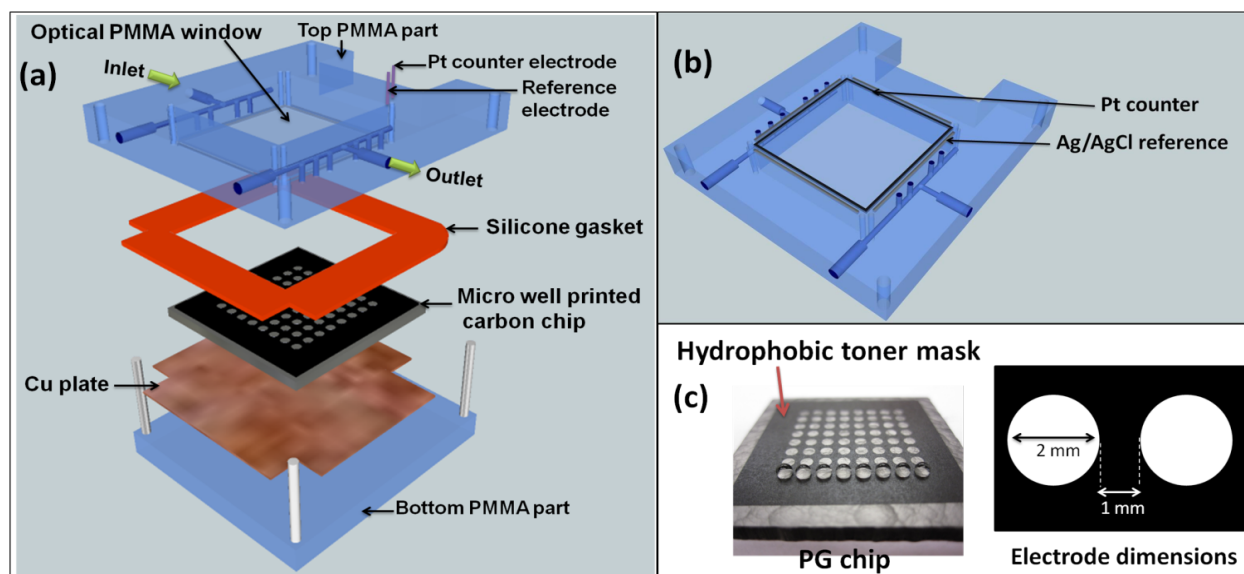


Figure S1 (a) Component assembly of ECL chip and the fluidic reaction chamber, (b) Underside view of reference and counter electrode wires in the top poly(methylmethacrylate) (PMMA) plate, (c) pyrolytic graphite (PG) chip with printed 1 μ L microwells. The first row is shown containing 1 μ L water droplets.

chip for electrical connection, and a bottom PMMA plate. The top PMMA plate was fabricated with 4 mm diameter female ports to connect to 0.2 mm i.d. polyether ether ketone (PEEK) tubing forming an inlet and an outlet. Pt counter and Ag/AgCl reference electrodes were partially embedded in grooves on the underside of the top PMMA plate (Scheme S1(b)). The hydrophobic mask to make microwells was designed with the software Inkscape on a 1:1 scale (Figure S1(c)). It was then printed onto high gloss paper (the backing of Avery labels) using an HP laser jet printer at 1200 dots per inch (dpi). The mask was then cut and transferred onto the bare PG by heating in a press at 290 °F for 90 s. Each well holds maximum of 1.5 ± 0.1 μ L volume of solution, and facilitates to construct the films containing enzymes, DNA and Ru^{II}-PVP. A flexible silicone gasket was placed on top of the microwell printed PG chip, and the entire assembly was sandwiched between the hard PMMA plates bolted together with screws (Figure S1(a)) to form a sealed fluidic channel. The ECL chip inlet port was connected to a dual syringe pump (55-3333, Harvard Inc.) via a 4-way switching valve (v101D, IDEX Inc) to direct buffers and reaction solutions into the device (Figure S1).

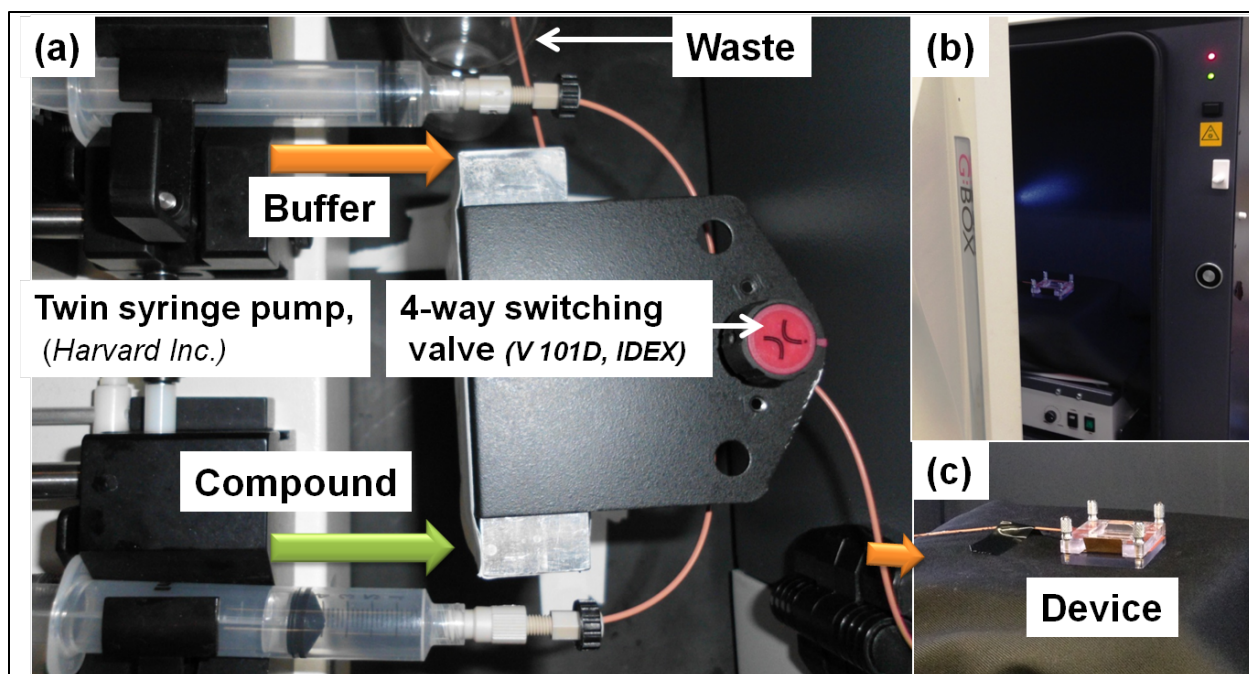


Figure S2 Device assembly for enzyme reactions and ECL acquisition, (a) Fluidic pumping system equipped with dual syringe pump and 4-way switching valve, which was used to direct wash buffer and B[a]P substrate solution into the device as necessary; (b) G:BOX (SynGene), ECL acquisition dark box and integrated CCD camera (CCD camera is positioned at top of the box to capture images, which is not shown in this figure); (c) the device is placed inside the box and connected with the pumping system by PEEK tubing.

Spot deposition

Enzyme/Ru^{II}PVP/DNA films were formed a layer at a time in the microwells using 1 μ L droplets of previously optimized solution compositions.^{3,4} Each adsorbate solution was sequentially incubated in the microwells for 20 min at 4 °C, washing with water between depositions, except 30 min incubations were used for enzymes and DNA. Solutions were (a) poly(diallyldimethylammonium) chloride (PDDA), 2 mg mL⁻¹ in 0.5 M NaCl; 3 mg mL⁻¹ in 0.5 M NaCl; (b) Ru^{II}PVP, 2.5 mg mL⁻¹ in 50% V/V ethanol; (c) calf thymus DNA, 2 mg mL⁻¹ in 10 mM TRIS + 0.5 M NaCl, pH 7.4; (d) human liver microsomes (Liver); (e) human lung microsomes (Lung); (f) human intestinal microsomes (Intestine); (g) human kidney microsomes (Kidney); (h) human liver cytosol (HLC); (i) Human lung cytosol (HLuC); (j) human intestinal cytosol (HIC); (k) human kidney cytosol (HKC). Supersomes were all expressed in baculovirus-insect cells and used as (a) cyt P450 1B1 supersomes (cyt P450 1B1), 4.5 mg mL⁻¹ in 100 mM potassium phosphate buffer of pH 7.4; (b) cyt P450 3A4 supersomes (cyt P450 3A4); (c) cyt P450 3A5 supersomes (cyt P450 3A5); (d) cyt P450 1A2 supersomes, (cyt P450 1A2). All LbL films have general film architecture, (Ru^{II}PVP/DNA)₂/ Ru^{II}PVP /human organ microsome or cyt P450 enzyme source/human organ cytosol or PDDA/DNA, where the first four analytical spots were deposited without cytosol, while the last four were with cytosol (Scheme 2).

Enzyme reaction and ECL signal acquisition

Enzyme reactions were run by flowing reactant solution (Styrene, NNK or 2-AAF) including necessary cofactors to facilitate conjugative reactions, (0.1 mM uridine 5'-diphospho-glucuronic acid, 0.1 mM Acetyl coenzyme A and 0.1 mM 3'-phosphoadenosine 5'-phosphosulfate) through the chip (Scheme 1) at $500 \mu\text{L min}^{-1}$ using constant potential of $-0.65 \text{ V vs. Ag/AgCl}$ (0.14 M KCl) at $22 (\pm 2) ^\circ\text{C}$ to activate natural cyt P450 catalysis as reported previously,⁵⁻⁸ followed by washing with anaerobic 50 mM phosphate buffer + 0.1 M NaCl of pH 7.4 for 3 min at $500 \mu\text{L min}^{-1}$. Then, $1.25 \text{ V vs. Ag/AgCl}$ was applied to the array for 180 s with a CHI 1232 electrochemical analyzer (CH Instruments Inc.) to generate ECL that is detected by the CCD camera.⁴ Signal integration and data analysis were done using Syngene Gene Tools v3.06 (SynGene), with color enhancement using Photoshop CS.

DNA-metabolite molecular profiling and quantitation by LC-MS/MS

100 μL PDDA was added dropwise followed by a 20-min incubation to a solution of 0.4 mg of magnetic particles dispersed in 100 μL of 5 mM Tris buffer (pH 7.0, 5 mM NaCl) to coat the negatively charged surface with positively charged polyions. After incubation, the supernatant was discarded and the particles were washed twice with Tris buffer to remove loosely bound polyions and redispersed in 100 μL of Tris buffer. In a similar fashion 50 μL of microsomes, cytosols, cyt P450 supersomes and DNA were incorporated with 30 min incubation for each to yield the general film architecture, Magnetic bead/PDDA/human organ microsome or cyt P450 enzyme source/human organ cytosol or PDDA/DNA. These magnetic particle bioreactors were dispersed in 10 mM phosphate buffer (pH 7.4) to a final volume of 200 μL and stored at $\sim 0 ^\circ\text{C}$ till use.

200 μL of magnetic bead bio colloidal suspension in 10 mM phosphate buffer (pH 7.4) was incubated with 1 mM styrene for 4 hours, 250 μM 2-AAF for 4 hours and 150 μM NNK for 18 hours separately in the presence of NADPH regeneration system (10 mM glucose 6-phosphate, 4 units of glucose-6-phosphate dehydrogenase, 10 mM MgCl_2 , 0.80 mM NADP^+ plus 0.1 mM uridine 5'-diphospho-glucuronic acid and 0.1 mM 3'-phosphoadenosine 5'-phosphosulfate) at $37 ^\circ\text{C}$ for metabolite generation and DNA adduct formation. Particles were then washed three times in Tris buffer to remove any unreacted compounds.

DNA adduct extraction was done by using neutral thermal hydrolysis or enzymatic hydrolysis depending on the DNA adduct stability. For neutral thermal hydrolysis the beads were re dispersed in 100 μL of ultrapure water and subjected to heat in a boiling water bath for 1 hour as described previously.⁹ $\text{O}^6\text{-POB-G}$ and $\text{N}^7\text{-Me-G}$ of NNK and Styrene-G adduct of styrene were extracted from the beads by neutral thermal hydrolysis. Enzymatic hydrolysis was done by incubating the beads with an enzyme system consists of deoxyribonuclease I (400 unit mg^{-1} of DNA), phosphodiesterase I from snake venom (0.2 unit mg^{-1} of DNA), phosphodiesterase II (0.01 unit mg^{-1} of DNA), nuclease P1 (5 units mg^{-1} DNA), 10 μL of 10 mM MgCl_2 , and phosphatase alkaline (1.2 unit mg^{-1} of DNA), for 12 h at $37 ^\circ\text{C}$. $\text{O}^6\text{-PHOB-G}$ and $\text{O}^6\text{-Me-G}$ of NNK and 2-AAF DNA adducts were treated with enzyme hydrolysis. Supernatants after extractions which contain DNA-metabolite adducts were separated from magnetic particle bioreactors and vacuum filtered in OmegaTM membrane filter and were spiked with 0.17 μM of 7-methylguanosine as an internal standard before LC-MS/MS analysis.

The DNA adduct analysis was performed using a capillary LC (Waters, Capillary LC-XE, Milford, MA) coupling with a 4000 QTRAP mass spectrometer (AB Sciex, Foster City, CA). For DNA adducts of 2-AAF, 10 μL of sample was injected into a Luna C18 trap column (0.5 mm \times 20mm, Phenomenex) and flushed at a flow rate of 10 $\mu\text{L min}^{-1}$ to eliminate the residual salt. After 3 min, the 10-port-valve switched from the loading position to eluting position and the adducts were flushed to a Luna C18 analytical column (0.5mm \times 150mm, Phenomenex) with A, ammonium acetate buffer (10 mM, pH 5.5 with 0.1% formic acid) and B, acetonitrile (with 0.1% formic acid). For DNA adducts of styrene and NNK, 10 μL of sample was directly loaded to the Luna C18 analytical column. The gradient for the sample separation in the analytical column followed the table below at a flow rate of 15 $\mu\text{L min}^{-1}$. The on-line mass spectrometer with Analyst 1.4 software was operated in the positive ion mode. Samples were analyzed in multiple reactions monitoring (MRM) mode at 5000 V ion spray voltage, 40 eV declustering potential, 25 eV collision energy and 0.15 s dwell time for each mass transitions.

Table S1 LC gradient used for separation.

NNK or Styrene		2-AAF	
Time (min)	B%	Time (min)	B%
0	5.0	0	10
4	5.0	5	10
24	35.0	15	40
28	35.0	35	40
29	5.0	37	10
30	5.0	40	10

Comet assay for results validation

A549, Caco-2, HEK 293 and Hep G2 cells (5×10^4 cells/well) were seeded on 12-well plates and cultured for 24 h at 37°C and 5% CO₂ in Dulbecco's Modified Eagle Medium (DMEM, 1 mL/well) containing 10% (v/v) fetal bovine serum, 2mM L-glutamine, 100 U/mL of penicillin and 0.1 mg/mL streptomycin. A monolayer of cells was then treated with 150 μM of the test compound 37°C for 24, 36, 48 and 60 hours. The cells were harvested and resuspended in Ca- and Mg-free PBS for the Comet Assay.

Comet assay was run by using OxiSelect™ Comet Assay kit (Cell Biolab, San Diego, CA). 10 μL of the cell suspension and 100 μL of low-melting agarose were mixed and 75 μL of the mixture was immediately pipetted onto the pre-warmed OxiSelect™ Comet Slide. The slides were maintained horizontally at 4°C in the dark for 15 minutes followed by immersion in pre-chilled lysis buffer (OxiSelect™ Comet Assay kit) at 4°C for 45 minutes in the dark. The slides were then immersed in a pre-chilled alkaline solution (pH>13) for 30 minutes in the dark. Slides were later transferred to electrophoresis chamber containing alkaline electrophoresis solution, and

electrophoresis was performed at 20V 300mA for 20min. After electrophoresis, the slides were washed with water twice, and then was immediately placed in 70% ethanol for 5 min and air-dried overnight at room temperature. Cells were stained with Vista Green DNA Dye®, dried, and images were recorded using an epifluorescent microscope (Zeiss Axiovert Widefield Microscope) with FITC filter. The images were analyzed by Comet Assay IV software from Perceptive Instruments Ltd (Bury St Edmunds, UK). Data were based on 50 randomly selected cells per sample. The tail migration has been considered to be an appropriated index of induced DNA damage.

Tail migration=Mean tail length.¹⁰

RESULTS

Film fabrication and characterization

The LbL assemblies of the films were constructed on 9 MHz QCM resonators (AT-cut, International Crystal Mfg.), where the gold electrodes were already functionalized with a monolayer of negatively-charged 3-Mercaptopropionic acid by incubating the resonators in 0.5 mM 3-Mercaptopropionic acid in ethanol overnight. The adsorption conditions and stability of each layer was optimized and frequency change (ΔF) was measured after washing with deionized water and drying over a stream of nitrogen. The mass per unit area M/A (g cm^{-2}) in each layer is related to ΔF , which is given by^{3,11}

$$M/A = -\Delta F(\text{Hz})/(1.83 \times 10^8) \quad (\text{S1})$$

where A is the area of the gold disk on the quartz resonator in cm^2 . Similarly nominal film thickness for films deposited on one side of the resonator, d (nm) is given by

$$d = -2(0.016 \pm 0.002)\Delta F(\text{Hz}) \quad (\text{S2})$$

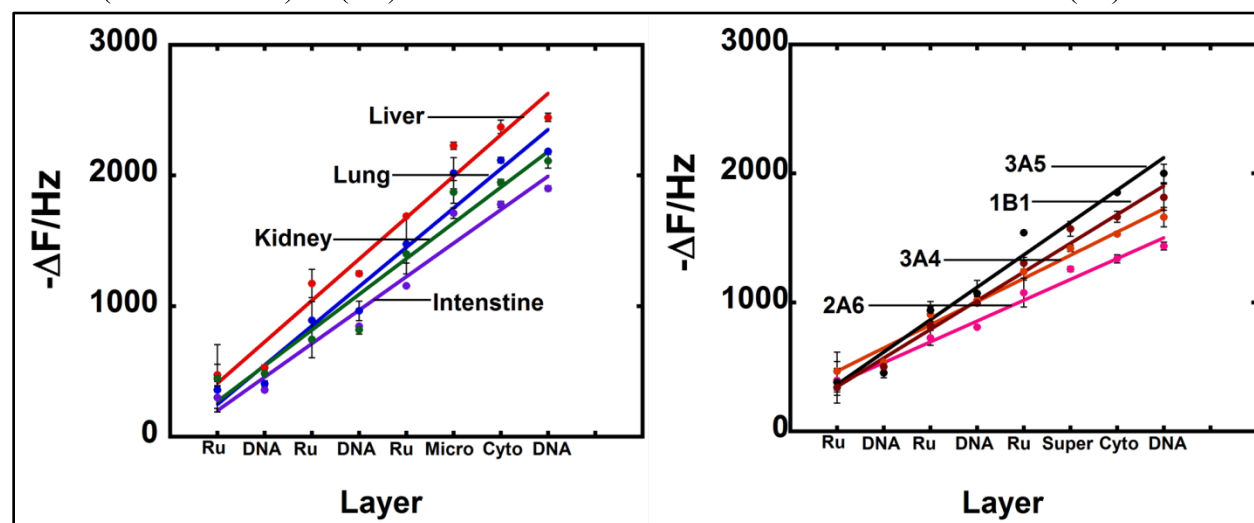


Figure S3 QCM frequency changes as a function of the number of adsorbed layers during the film growth. Error bars reflect SD for 3 resonators. Ru - Ru^{II}PVP, Micro- human organ microsome, Cyto – human organ cytosol, and Super- human organ supersome.

Table S2 Characteristics of the films.

Film assembly	Liver	Lung	Intestine	Kidney	3A4	2A6	3A5	1B1
Nominal thickness / nm	78	70	60	68	54	56	64	58
Mass density of RuPVP / $\mu\text{g cm}^{-2}$	8.5 \pm 0.9	7.5 \pm 0.7	5.4 \pm 0.9	6.9 \pm 0.6	6.3 \pm 0.3	5.8 \pm 0.6	8.4 \pm 0.5	6.4 \pm 0.3
Mass density of DNA / $\mu\text{g cm}^{-2}$	1.2 \pm 0.2	1.1 \pm 0.8	1.5 \pm 0.4	1.5 \pm 0.7	1.7 \pm 0.6	1.3 \pm 0.4	1.9 \pm 0.2	2.6 \pm 0.6
Mass density of cyt P450 source / $\mu\text{g cm}^{-2}$	2.9 \pm 0.5	2.9 \pm 0.6	3.0 \pm 0.7	2.6 \pm 0.5	0.4 \pm 0.5	0.4 \pm 0.5	0.4 \pm 0.5	0.4 \pm 0.2
Mass density of cytosol / μgcm^{-2}	0.8 \pm 0.2	0.6 \pm 0.1	0.4 \pm 0.1	0.4 \pm 0.2	0.6 \pm 0.3	0.4 \pm 0.4	0.8 \pm 0.1	0.5 \pm 0.1

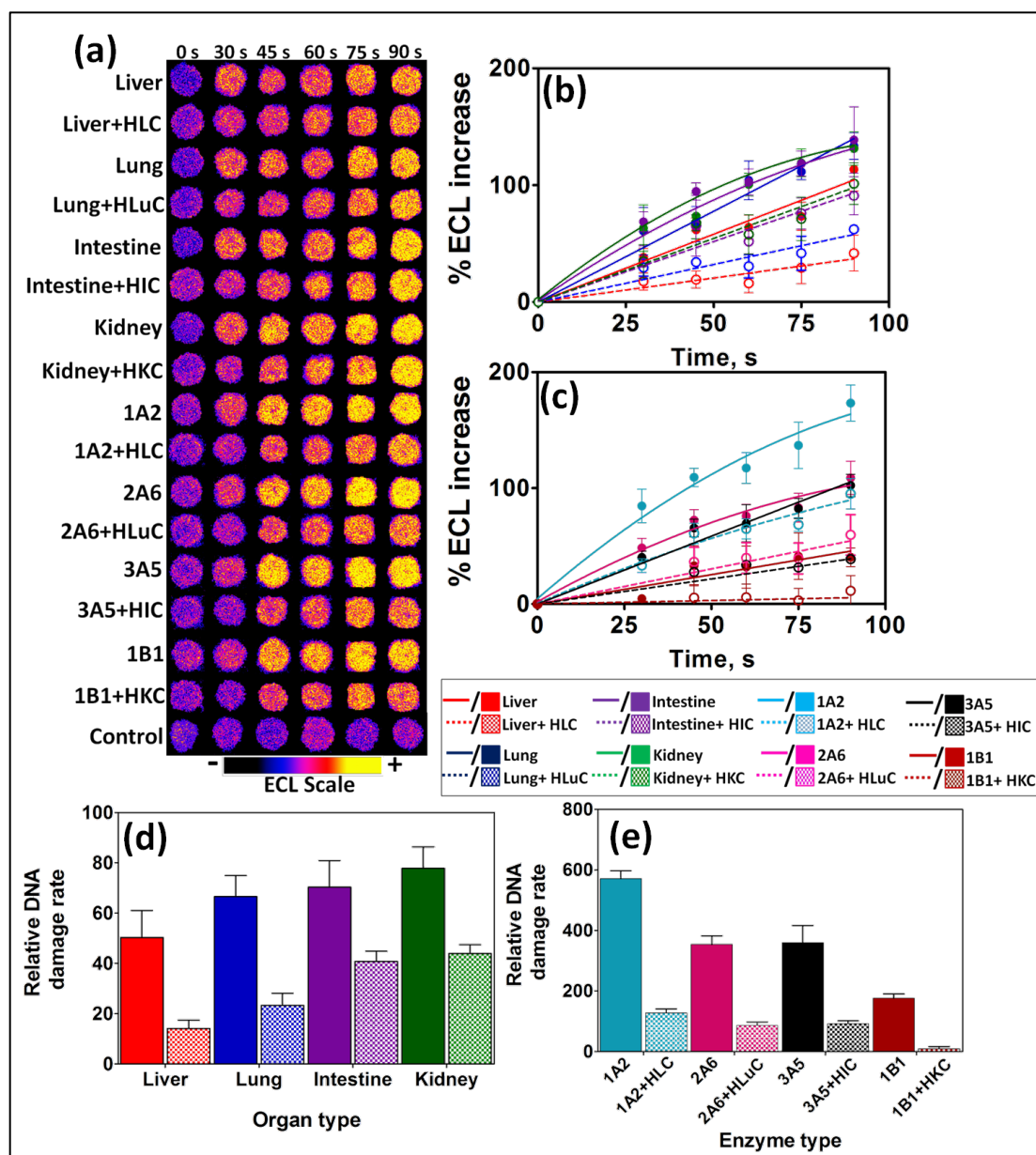


Figure S4: ECL array data from spots containing optimized Ru^{II}PVP/enzyme/DNA film assemblies reacted with oxygenated 250 μ M of 2-AAF in pH = 7.4 phosphate buffer + necessary cofactors with bioelectronic activation of cyt P450s at -0.65 V vs. Ag/AgCl (0.14 M KCl) for reaction times from 0–90 s. (a) Reconstructed and recolored ECL array images. Control spots contained liver microsomes, and were subjected to the same reaction conditions as above without exposure to 2-AAF. Influence of enzyme reaction time on % ECL increase for fluidic sensor chips reacted with 250 μ M of 2-AAF in pH = 7.4, (b) with human organ tissue fractions, (c) with cyt P450 isoforms, where error bars represent standard deviations for $n = 4$. The relative DNA damage rate ($\{\text{mg of protein}\}^{-1} \text{s}^{-1} \text{mM}^{-1}$) upon exposure to 2-AAF at analytical spots containing (d) human organ tissue fractions, (e) cyt P450 supersomes.

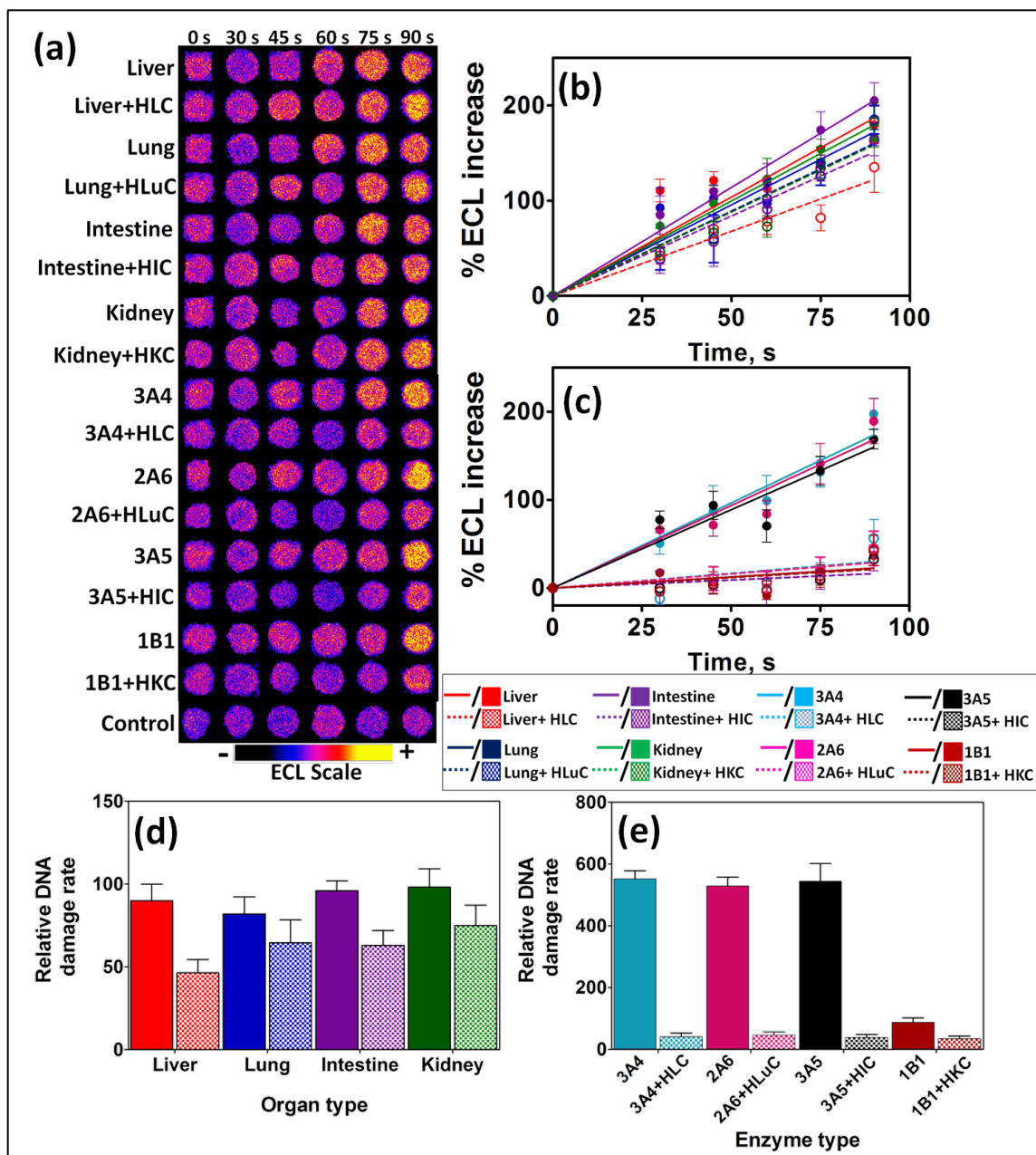


Figure S5: ECL array data from spots containing optimized $\text{Ru}^{\text{II}}\text{PVP}/\text{enzyme}/\text{DNA}$ film assemblies reacted with oxygenated 1 mM of styrene in pH = 7.4 phosphate buffer + necessary cofactors with bioelectronic activation of cyt P450s at -0.65 V vs. Ag/AgCl (0.14 M KCl) for reaction times from 0–90 s. (a) Reconstructed and recolorized ECL array images. Control spots contained liver microsomes, and were subjected to the same reaction conditions as above without exposure to 2-AAF. Influence of enzyme reaction time on % ECL increase for fluidic sensor chips reacted with 1 mM of styrene in pH = 7.4, (b) with human organ tissue fractions, (c) with cyt P450 isoforms, where error bars represent standard deviations for $n = 4$. The relative DNA damage rate ($\{\mu\text{g of protein}\}^{-1} \text{ s}^{-1} \text{ mM}^{-1}$) upon exposure to styrene at analytical spots containing (d) human organ tissue fractions, (e) cyt P450 supersomes.

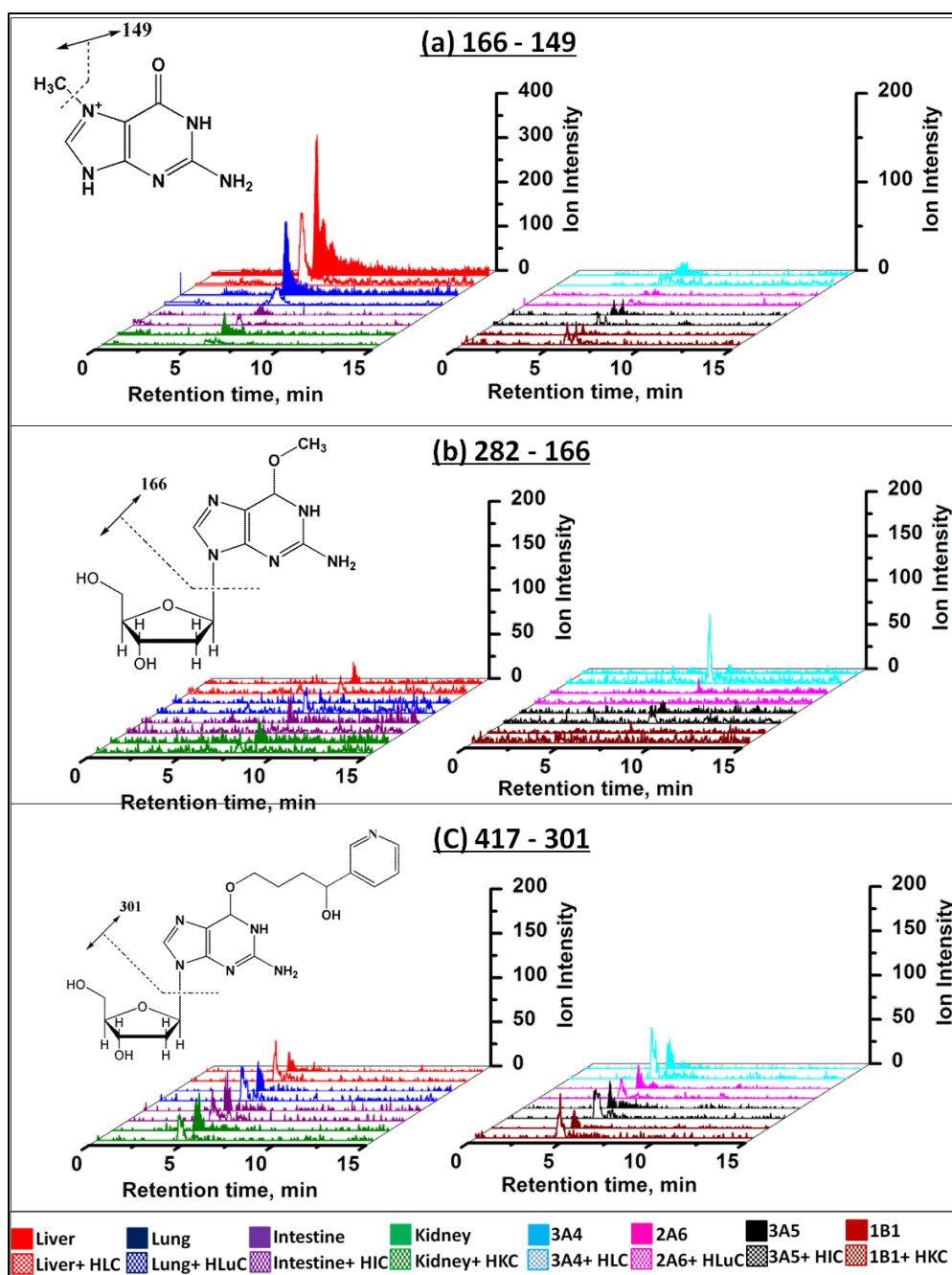


Figure S6: Single reaction monitoring (SRM) chromatograms for m/z transitions (a) 166-149 monitoring formation of N^7 -Methyl-guanine adducts (**3**, Scheme 4), (b) 282-166 of O^6 -Methyl-guanine adducts (**2**, Scheme 4) and (c) 417-301 of O^6 -Pyridylhyoxybutyl-guanine (**5**, Scheme 4) from biocolloid reactors (color code link on bottom) containing human organ microsomes and cyt P450 supersomes reacted with 150 μ M NNK.

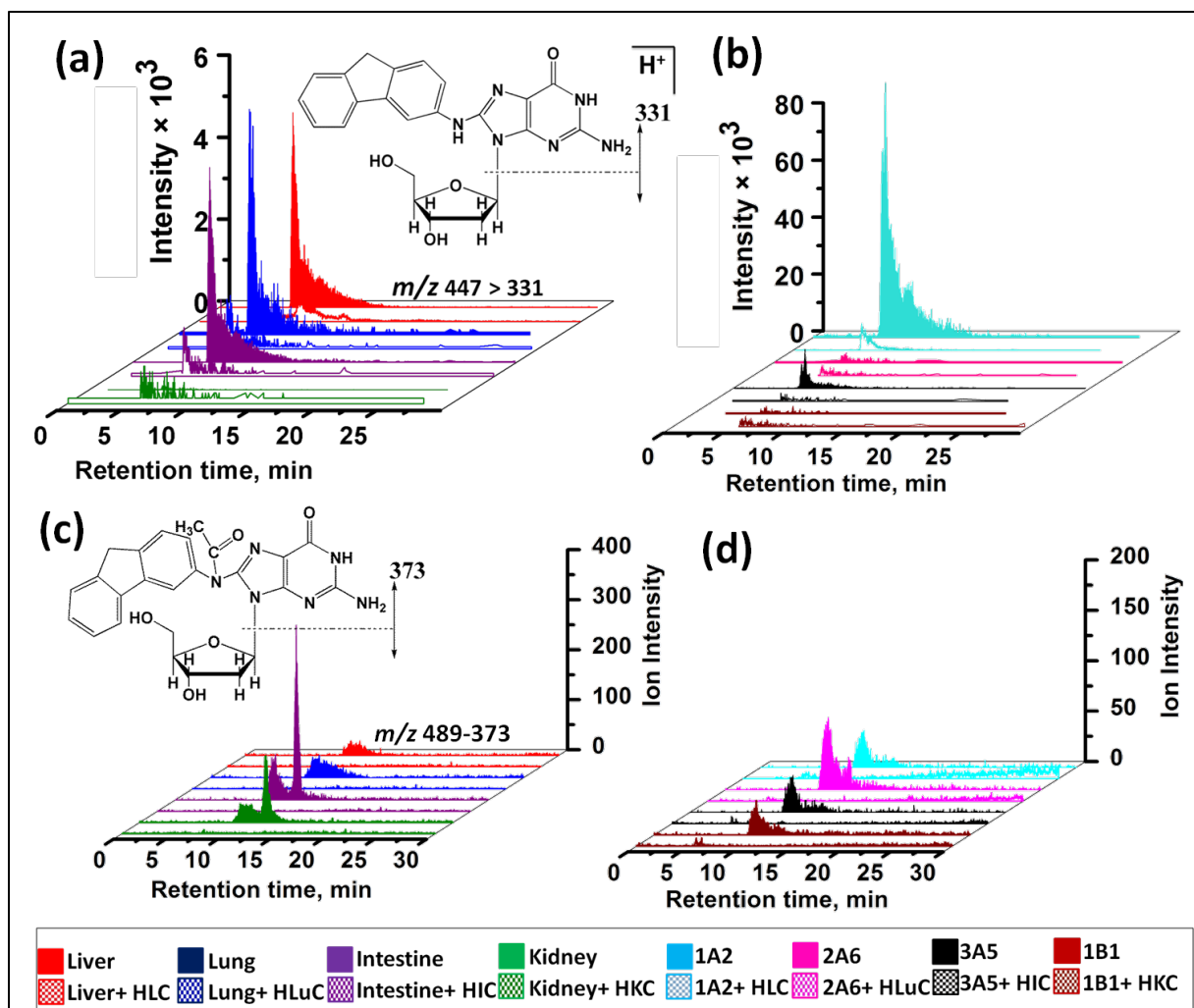


Figure S7: Single reaction monitoring (SRM) chromatograms monitoring formation of DNA adducts by biocolloid reactors (color code link on bottom) after reaction with 250 μ M 2-AAF at pH = 7.4 for 4 hrs; (a) *m/z* transition 447-331 of N-(Deoxygunaosin-8-yl)-2-aminofluorene (8, Scheme 5) adducts from biocolloid reactors containing human organ microsomes, (b) cyt P450 supersomes. Panels (c) and (d) show SRM chromatogram for *m/z* transition 489-373 monitoring formation of N-(Deoxygunaosin-8-yl)-2-acetylaminofluorene (9, Scheme 5) (c) human organ microsomes, (d) cyt P450 supersomes.

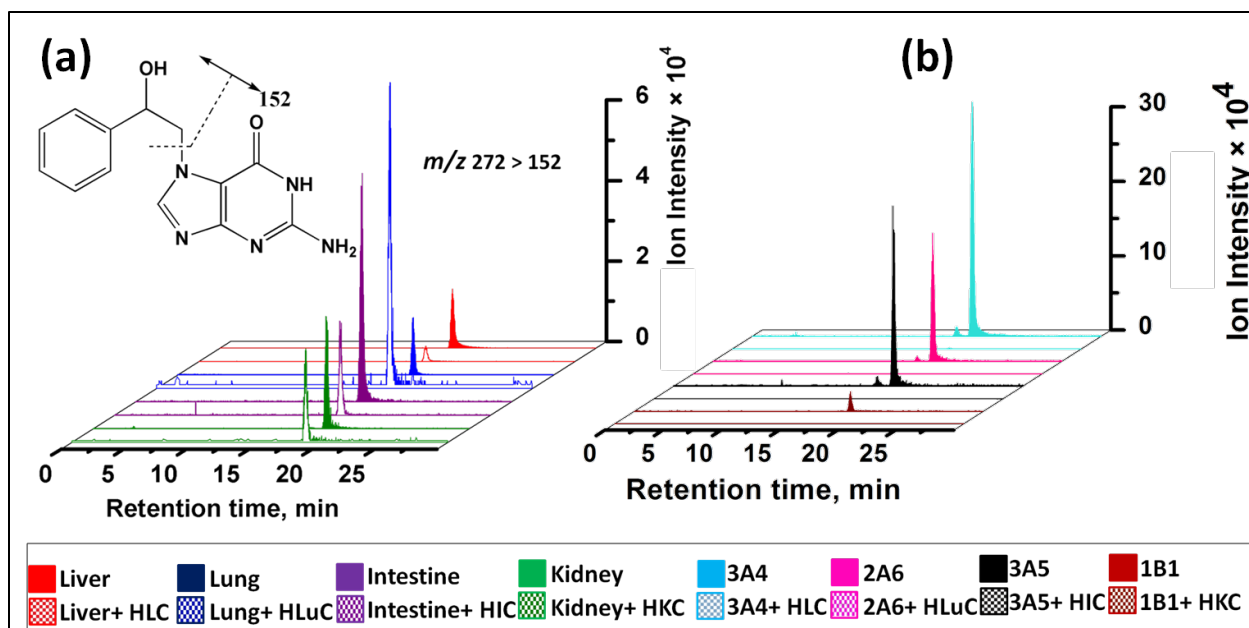


Figure S8: Single reaction monitoring (SRM) chromatogram for m/z transition 272-152 monitoring formation of N^7 styrene oxide guanine adduct (**10**, Scheme 6) from biocolloid reactors (color code link on bottom) containing (a) human organ microsomes, (b) cyt P450 supersomes.

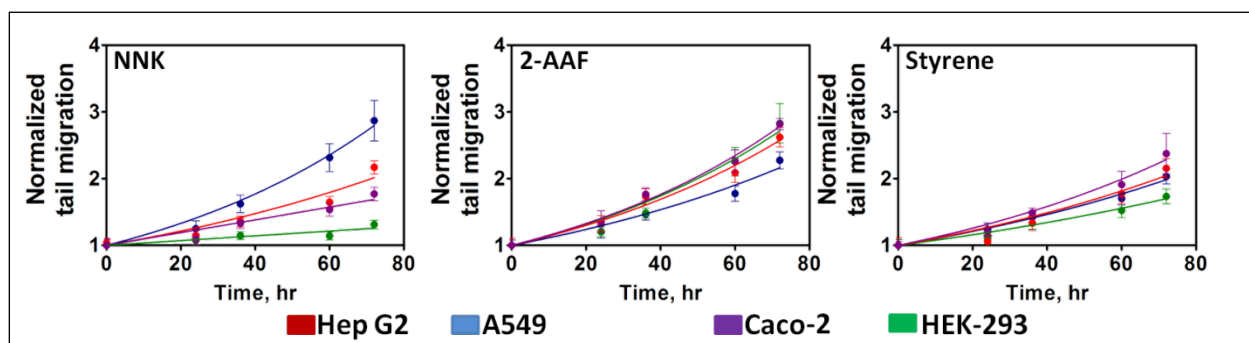


Figure S9: Influence of reaction time on normalized tail migration (tail migration, hr^{-1}) of treated cells (Color code at the bottom) for the compounds, NNK, 2-AAF and styrene.

Table S3: DNA adducts (pmol {microgram of protein}⁻¹ {mM of NNK}⁻¹) formed by biocolloid reactors after reaction with 150 μM NNK at pH = 7.4 for 18 hrs.

Enzyme source	Amount of DNA adducts (pmol {microgram of protein} ⁻¹ {mM of NNK} ⁻¹)			
	Adduct 4	Adduct 5	Adduct 2	Adduct 3
HLM	7.12 ± 0.18	0.45 ± 0.04	0.3 ± 0.01	1.94 ± 0.02
HLM+HLC	5.85 ± 1.00	0.51 ± 0.04	0.22 ± 0.01	0.93 ± 0.01
HLuM	13.07 ± 0.70	0.52 ± 0.08	0.16 ± 0.01	0.87 ± 0.04
HLuM+HLuC	8.85 ± 1.44	0.74 ± 0.04	0.45 ± 0.01	0.54 ± 0.05
HIM	7.89 ± 0.43	0.71 ± 0.13	0.54 ± 0.01	0.36 ± 0.02
HIM+HIC	4.36 ± 0.31	0.81 ± 0.11	0.32 ± 0.03	0.14 ± 0.01
HKM	0.00 ± 0.00	0.68 ± 0.05	0.21 ± 0.01	0.13 ± 0.08
HKM+HKC	0.00 ± 0.00	0.67 ± 0.01	0.14 ± 0.03	0.07 ± 0.04
cyt P450 3A4	111.14 ± 13.90	0.61 ± 0.02	0.20 ± 0.01	0.26 ± 0.01
cyt P450 3A4+HLC	28.76 ± 6.87	0.89 ± 0.09	0.87 ± 0.04	0.15 ± 0.02
cyt P450 2A6	263.13 ± 15.90	0.51 ± 0.02	0.20 ± 0.01	0.07 ± 0.01
cyt P450 2A6+HLuC	77.51 ± 6.88	0.45 ± 0.06	0.12 ± 0.01	0.06 ± 0.04
cyt P450 3A5	115.42 ± 8.68	0.67 ± 0.03	0.27 ± 0.02	0.05 ± 0.01
cyt P450 3A5+HIC	68.33 ± 11.70	0.82 ± 0.08	0.28 ± 0.02	0.06 ± 0.01
cyt P450 1B1	0.20 ± 0.11	0.45 ± 0.05	0.12 ± 0.02	0.05 ± 0.01
cyt P450 1B1+HKC	0.06 ± 0.02	0.65 ± 0.09	0.11 ± 0.01	0.06 ± 0.01

Table S4: DNA adducts (pmol {microgram of protein}⁻¹ {mM of 2-AAF}⁻¹) formed by biocolloid reactors after reaction with 250 μM 2-AAF at pH = 7.4 for 4 hrs.

Enzyme source	Amount of DNA adducts (pmol {microgram of protein} ⁻¹ {mM of 2-AAF} ⁻¹)	
	Adduct 8	Adduct 9
HLM	0.54 ± 0.15	0.15 ± 0.17
HLM+HLC	0.22 ± 0.06	N.D.
HLuM	0.39 ± 0.04	0.06 ± 0.02
HLuM+HLuC	0.49 ± 0.09	N.D.
HIM	0.42 ± 0.07	0.76 ± 0.33
HIM+HIC	0.41 ± 0.19	N.D.
HKM	0.43 ± 0.04	0.39 ± 0.03
HKM+HKC	0.18 ± 0.07	N.D.
cyt P450 1A2	4.45 ± 0.65	0.23 ± 0.16
cyt P450 1A2+HLC	0.70 ± 0.44	N.D.
cyt P450 2A6	0.82 ± 0.35	0.17 ± 0.07
cyt P450 2A6+HLuC	0.87 ± 0.36	N.D.
cyt P450 3A5	0.69 ± 0.30	0.15 ± 0.05
cyt P450 3A5+HIC	0.65 ± 0.27	N.D.
cyt P450 1B1	0.08 ± 0.01	0.30 ± 0.03
cyt P450 1B1+HKC	0.09 ± 0.04	N.D.

Note:- N.D. Not detectable

Table S5: T-test values, t_{cal} - Calculated t value, t_{tab} - Critical two-tailed t value for n=4 at 95% confidence interval = 3.182.¹² If the value in the table below is >3.185, the two relevant sets of data are significantly different at the 95% confidence level (P=0.5). Green highlighted labels reflect data averages that are not significantly different. A: without cytosol & B: with cytosol.

t_{cal}						
Styrene						
	Liver vs Lung	Liver vs Intestine	Liver vs Kidney	Lung vs Intestine	Lung vs Kidney	Intestine vs Kidney
A	1.08	0.95	1.08	2.25	2.15	0.36
B	2.23	2.63	3.15	0.20	1.11	1.55
	3A4 vs 2A6	3A4 vs 3A5	3A4 vs 1B1	2A6 vs 3A5	2A6 vs 1B1	3A5 vs 1B1
A	1.22	0.26	32.06	0.48	28.14	15.61
B	0.69	0.20	0.75	1.04	1.73	0.65
2-AAF						
	Liver vs Lung	Liver vs Intestine	Liver vs Kidney	Lung vs Intestine	Lung vs Kidney	Intestine vs Kidney
A	2.39	0.35	4.01	0.56	1.89	1.11
B	3.15	10.09	12.40	5.55	6.99	1.18
	1A2 vs 2A6	1A2 vs 3A5	1A2 vs 1B1	2A6 vs 3A5	2A6 vs 1B1	3A5 vs 1B1
A	11.37	6.79	27.18	0.17	11.29	6.24
B	4.92	4.43	15.57	0.74	11.86	13.32
NNK						
	Liver vs Lung	Liver vs Intestine	Liver vs Kidney	Lung vs Intestine	Lung vs Kidney	Intestine vs Kidney
A	12.49	7.29	8.84	9.35	18.72	19.39
B	4.67	2.26	7.07	13.98	24.70	14.44
	3A4 vs 2A6	3A4 vs 3A5	3A4 vs 1B1	2A6 vs 3A5	2A6 vs 1B1	3A5 vs 1B1
A	6.84	2.87	15.19	8.39	16.48	10.57
B	5.43	1.91	13.62	7.06	16.43	12.08

REFERENCE

- (1) (a) L. Dennany, R. J. Forster, and J. F. Rusling, *J. Am. Chem. Soc.*, 2003, **125**, 5213–5218; (b) G. C. Jensen, and E. G. Hvastkovs, Facile One Pot Preparation of Ru(bpy)₂(PVP)₁₀]²⁺ (Ru^{II}PVP) metallopolymer, http://web2.uconn.edu/rusling/RuPVP_modified.pdf
- (2) R. Sato, and T. Omura, *J. Biol. Chem.*, 1964, **239**, 2370-2378.
- (3) Y. Lvov, in *Handbook of Surfaces and Interfaces of Materials*, ed. R. W. Nalwa, Academic Press, San Diego, CA, 2001, Vol. 3, pp 170-189.

-
- (4) D. P. Wasalathanthri, S. Malla, I. Bist, C. K. Tang, R. C. Faria, and J. F. Rusling, *Lab Chip*, 2013, **13**, 4554-4562.
- (5) S. Krishnan, J. B. Schenkman, and J. F. Rusling, *J. Phys. Chem. B*, 2011, **115**, 8371–8380.
- (6) S. Krishnan, D. Wasalathanthri, L. Zhao, J. B. Schenkman, and J. F. Rusling, *J. Am. Chem. Soc.*, 2011, **133**, 1459–1465.
- (7) D. P. Wasalathanthri, S. Malla, R. C. Faria, J. F. Rusling, *Electroanalysis*, 2012, **24**, 2049-2052.
- (8) D. P. Wasalathanthri, V. Mani, C. K. Tang, and J. F. Rusling, *Anal. Chem.*, 2011, **83**, 9499–9506.
- (9) M. Tarun, and J. F. Rusling, *Crit. Rev. Eukaryotic Gene Expression* 2005, **15**, 295-315
- (10) www.perceptive.co.uk/cometassay/†
- (11) Y. Lvov, K. Ariga, I. Ichinose, and T. Kunitake, *J. Am. Chem. Soc.*, 1995, 6117–6123.
- (12) S. L. Ellison, V. J. Barwick, and T. J. Farrat, in *Practical Statistics for the Analytical Scientist*, The Royal Society of Chemistry, Cambridge, U.K., 2009, pp 211.